Peptide insertion, positioning, and stabilization in a membrane: Insight from an all-atom molecular dynamics simulation

ARTICLE *in* BIOPOLYMERS · APRIL 2007

Impact Factor: 2.39 · DOI: 10.1002/bip.20698 · Source: PubMed

5 AUTHORS, INCLUDING:

Alemayehu A Gorfe
University of Texas Medical School at Houston
75 PUBLICATIONS **1,670** CITATIONS
SEE PROFILE

Judy Kim
Villanova University
42 PUBLICATIONS **844** CITATIONS
SEE PROFILE

Peptide Insertion, Positioning, and Stabilization in a Membrane: Insight from an All-Atom Molecular Dynamics Simulation

Arneh Babakhani,[1] Alemayehu A. Gorfe,[1] Justin Gullingsrud,[1] Judy E. Kim,[1] J. Andrew McCammon[1,2,3]

[1] *Department of Chemistry & Biochemistry, University of California at San Diego, La Jolla, CA 92093-0365*

[2] *Department of Pharmacology, University of California at San Diego, La Jolla, CA 92093-0365*

[3] *Howard Hughes Medical Institute, University of California at San Diego, La Jolla, CA 92093-0365*

Received 22 November 2006; revised 23 January 2007; accepted 29 January 2007
Published online 1 February 2007 in Wiley InterScience (www.interscience.wiley.com). DOI 10.1002/bip.20698

ABSTRACT:

Peptide insertion, positioning, and stabilization in a model membrane are probed via an all-atom molecular dynamics (MD) simulation. One peptide (WL5) is simulated in each leaflet of a solvated dimyristoylglycero-3-phosphate (DMPC) membrane. Within the first 5 ns, the peptides spontaneously insert into the membrane and then stabilize during the remaining 70 ns of simulation time. In both leaflets, the peptides localize to the membrane interface, and this localization is attributed to the formation of peptide–lipid hydrogen bonds. We show that the single tryptophan residue in each peptide contributes significantly to these hydrogen bonds; specifically, the nitrogen heteroatom of the indole ring plays a critical role. The tilt angles of the indole rings relative to the membrane normal in the upper and lower leaflets are approximately 26° and 54°, respectively. The tilt angles of the entire peptide chain are 62° and 74°. The membrane induces conformations of the peptide that are characteristic of β-sheets, and the peptide enhances the lipid ordering in the membrane. Finally, the diffusion rate of the peptides in the membrane plane is calculated (based on experimental peptide concentrations) to be approximately 6 Å^2/ns, thus suggesting a 500 ns time scale for intermolecular interactions. © 2007 Wiley Periodicals, Inc. Biopolymers 85: 490–497, 2007.

Keywords: transmembrane proteins; molecular dynamics simulation; membrane simulation; WL5; tryptophan localization

Correspondence to: Arneh Babakhani; e-mail: ababakha@mccammon.ucsd.edu
Contract grant sponsor: Howard Hughes Medical Institute
Contract grant sponsor: NSF
Contract grant sponsor: NIH
Contract grant sponsor: The Center for Theoretical Biological Physics
Contract grant sponsor: The National Biomedical Computation Resource
Contract grant sponsor: Commission for the Promotion of Young Academics, University of Zurich

This article was originally published online as an accepted preprint. The "Published Online" date corresponds to the preprint version. You can request a copy of the preprint by emailing the Biopolymers editorial office at biopolymers@wiley.com

INTRODUCTION

A wide range of functions, such as proton transport and cell signaling, illustrate the importance of transmembrane proteins in biological phenomena. Consequently, elucidating the chemical and biochemical behavior of these proteins is the subject of much research. For example, extensive spectroscopic techniques have been used to probe the relationship between the structure and function of transmembrane proteins.[1] Properties such as helix tilt angles, side chain orientations, and functional conformations have been studied in a variety of transmembrane proteins using NMR and Raman spectroscopy.[2–4] Tryptophan fluorescence and circular dichroism techniques have also been used to study the equilibrium penetration depth of small transmembrane peptides.[5]

Computational methods—including implicit membrane models, coarse-grained, and all-atom molecular dynamics (MD) simulations—have complemented experimental techniques. In the implicit membrane approach, the membrane is represented by an electrostatic continuum (such as the Generalized Born model) while the protein is treated explicitly.[6] This technique reduces the computational time required to model protein–membrane phenomena but does so at the expense of relevant details regarding the membrane. In coarse-grained modeling, two or more atoms can be merged to form a single bead; for instance, all of the phosphate atoms of a lipid head group can be represented by one bead, while the choline group atoms by a second bead.[7–9] This approach strives to employ the simplest possible description of its system components in order to gain specific physical insight, such as the conformational dynamics of a channel transmembrane protein.[10] As a result, coarse-grained modeling can provide insight on reactions that occur on relatively long biological time scales.

In contrast to implicit and coarse-grained modeling approaches, the all-atom MD method—in which nearly every atom is treated explicitly—can employ broadly transferable and accurate force fields describing the interactions between lipid, protein, and water. As an example, Aliste et al. employed all-atom MD simulations to study the thermodynamics of small peptides at a membrane–solvent interface.[11] In this study, the authors attempted to reproduce the Wimley–White scale,[12] which provides the free energy associated with the transfer of a residue from the solvent to the membrane. Although Aliste et al. were not completely successful in this endeavor, they successfully elucidated the energetic differences for peptide partitioning into a nonpolar solvent or a membrane. They also demonstrated that the penetration depth of the peptide into a membrane is a function of the peptide's hydrophobicity.

Protein insertion and positioning in a membrane host are of particular interest in transmembrane peptides. As experimental approaches continue to expand in this area,[13,14] computational approaches are also being used to reveal the details of protein insertion and positioning. Gorfe et al.[15] used all-atom MD to study the insertion and stabilization of a lipidated peptide. In their simulations, the authors applied an artificial force on the lipidated peptide to induce the insertion process. Once inserted, the applied force was turned off, and the lipidated peptide was allowed to stabilize. This nonequilibrium approach—also known as steered MD (SMD)—was used to enhance the rate of insertion. This technique is valid as long as the applied force does not significantly perturb the physical properties of the model membrane during the simulation.[16] If the thickness, order parameters, or cross-sectional area of the membrane are dramatically altered as the peptide inserts into the membrane, the SMD simulation is considered unrealistic. For this reason, care must be taken in selecting the magnitude of the pulling force. In addition to using realistic forces, an equilibrium, all-atom MD simulation of biomolecular insertion into a membrane is challenging because of the time scale; protein insertion requires microsecond to millisecond simulations, which are currently inaccessible by all-atom MD.[17]

In this study, we present an equilibrium all-atom MD simulation—with no biasing force—of a solvated peptide membrane system. The peptide used is WL5 and consists of one tryptophan (TRP) residue followed by five leucines. It is acetylated and amidated at its N- and C-termini, respectively. The membrane of choice is a 1,2-dimyristoylglycero-3-phosphocholine (DMPC) bilayer. We chose this small peptide in hopes of observing its spontaneous insertion into the membrane during an equilibrium MD study. The available experimental work on this system shows that multiple units of WL5 assemble in the membrane to form a multimeric antiparallel β-sheet.[18–20] While the experimental data will help validate the simulation results presented here, the latter will provide important atomic-level details and hence shed additional light on the phenomena of peptide insertion, positioning, and stabilization in the membrane host.

METHODS

A single WL5 peptide was assembled in an extended conformation using SYBYL.[21] Using the GROMACS MD package,[22] the peptide was placed by itself in a 25 nm^3 cubic box and solvated with 4092 water molecules. The peptide was held fixed in position and the water molecules were energetically minimized. This minimization scheme consisted of 2500 steps of steepest descent followed by 2500 steps of conjugate gradient minimization. The peptide was then liberated and the entire free system was again minimized by the same scheme. While restraining the heavy atoms of the peptide (with a force constant of 1000 kJ mol^{-1} nm^{-1}), the system was heated to a temperature of 310 K over 50 ps. Pressure coupling was then included, the restraints were lifted, and the free system of peptide in water was equilibrated for 5 ns. The last snapshot of the peptide (still in its extended form) was used as the starting conformation in the membrane/peptide simulation. A preequilibrated, 128-lipid DMPC membrane was obtained from the Tieleman laboratory.[11,23] To ensure the integrity of the membrane, it was further equilibrated in solvent for 10 ns. No appreciable change in the membrane thickness, order parameters, or area per lipid occurred (data not shown).

Using VMD,[24] one copy of the equilibrated peptide was situated on either side of the equilibrated bilayer, at an average distance of 10 Å from the nearest lipid head groups. The principal axis of the peptide was oriented parallel to the membrane plane, which was set to be the *xy*-plane. Using GROMACS, the system was placed in a box of dimensions 6.02 × 6.02 × 9.50 nm and then solvated with

6631 water molecules. The peptides and membrane were held fixed in position, while the water molecules were minimized via 2500 steps of steepest descent then 2500 steps of conjugate gradient minimization. The peptides and membrane were then liberated, and this entire free system was again minimized by the same scheme. The heavy atoms of the peptides and membrane were then restrained in position (force constant of 1000 kJ mol^{-1} nm^{-1}), while the solvent was heated to 310 K, over 50 ps. Finally, all restraints were removed, and the all-atom MD simulation (25,925 atoms) was conducted for a total of 75 ns.

The GROMOS (ffgmx) force field parameters were used for the peptides and solvent, while the lipid parameters provided by Berger et al.[25] were employed for the DMPC lipids. A time step of 2 fs and a nonbonded cutoff of 1.0 nm (for van der Waals interactions) were used. Full electrostatics were calculated using the particle mesh Ewald (PME) method, with sixth-order spline interpolation and a tolerance of 1×10^{-5}.[26,27] Berendsen temperature coupling was used,[28] with a reference temperature of 310 K and a coupling of 0.1 ps. For the production run, a semi-isotropic pressure coupling scheme was used, with a reference pressure of 1.0 bar, a pressure coupling of 0.5 ps, and a compressibility of 4.5×10^{-5} bar^{-1}. Trajectories were analyzed using the various GROMACS tools. Rendering and visualization were done in VMD. Plots and figures were created in MATLAB©.[29]

RESULTS AND DISCUSSION

Peptide Insertion and Positioning

During the first 5 ns of the production run, the peptide on either side of the membrane diffuses throughout the simulation box and associates with the membrane. The peptides then spend the remaining 70 ns of simulation time stabilizing in the membrane host (see Figure 1), consistent with the known thermodynamics of the system. The solute (peptide) is very hydrophobic and initially resides in a polar solvent. The head group region of the membrane is less polar,[30] and the local dielectric constant of the membrane core varies between 2 and 5.[31,32] Thus, as expected, the membrane serves as a thermodynamically favorable environment for the model peptide. Despite changes in their conformation and lateral positions, the peptides remain in the membrane for the duration of the simulation (as discussed below).

Shown in Figure 2 are the penetration depths of the peptides in each leaflet of the membrane. When averaged over 50 ps blocks during the last half of the simulation, the penetration depth of the peptide into the upper leaflet is 2.70 ± 1.05 Å. The corresponding depth in the lower leaflet is 1.26 ± 1.47 Å. The peptide in the upper leaflet resulted in a slightly more convergent result. The penetration depths in both leaflets are in agreement with each other, consistent with the symmetrical nature of the system. This observed penetration demonstrates the spontaneous insertion of the peptides, without the need for an external biasing force.

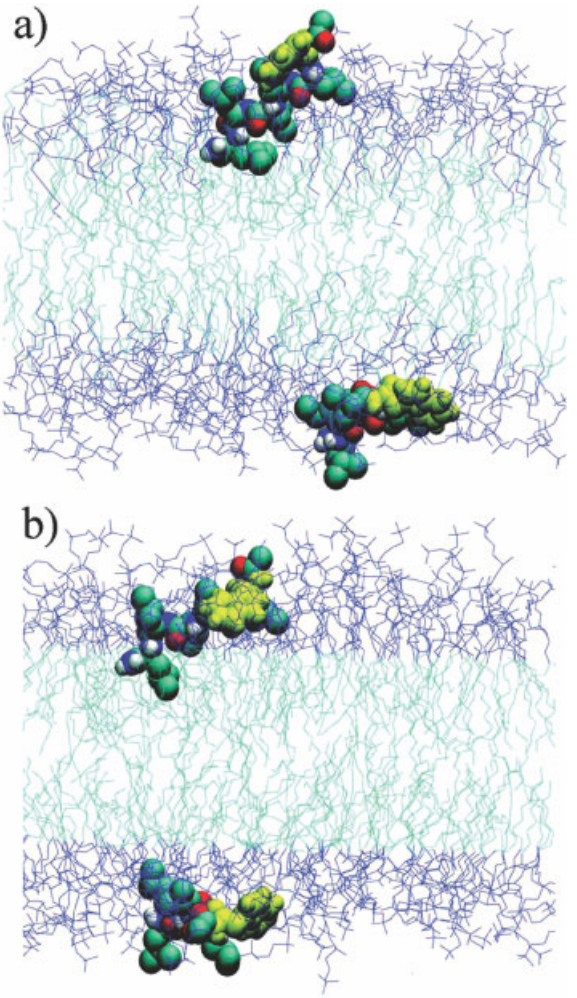

FIGURE 1 Simulation snapshots at (a) 25 ns and (b) 50 ns. Lipid head groups and tails are colored in dark blue and light green, respectively. Peptides are shown in the van der Waals representation, colored by atom (carbon = light green, nitrogen = dark blue, white = hydrogen, red = oxygen). The entire TRP residue in each peptide is colored yellow. Water molecules are omitted for clarity.

A noteworthy observation is that despite their hydrophobic nature, the peptides do not completely submerge into the membrane core. On our time scale, they stabilize at the membrane interface—a region defined to contain the first solvation layers, the lipid head groups, and the beginning of the lipid tails. This interfacial localization of the peptides can be ascribed to the tryptophan residue, as noted previously.[33] Yau et al. observe that the role of TRP in anchoring proteins to the interfacial region of membranes can be attributed to the physical characteristics of the indole side chain. Relevant characteristics of the indole group include the propensity of the indole nitrogen for hydrogen bonding and the orientation of the indole ring in the membrane host.

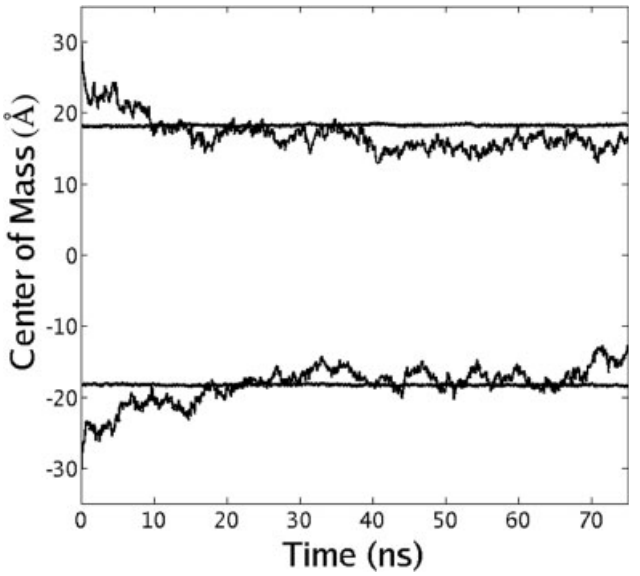

FIGURE 2 Position along the membrane normal vector (*z*-axis) of the peptide centers of mass as a function of time. Horizontal lines represent the position of the phosphorus atoms in the lipid head groups. The membrane is centered on the zero position; thus, profiles in the positive and negative zones correspond to the upper and lower membrane leaflets, respectively.

The TRP residue contributes significantly to the hydrogen bonding interactions of the entire peptide. Averaging over the entire course of the simulation (see Figure 3a), we find that TRP accounts for approximately 43% of the total peptide–membrane hydrogen bonds in the upper leaflet and 14% in the lower; thus, the TRP residue contributes significantly more to the hydrogen bonding in the upper leaflet of the membrane. Considering that TRP harbors only 3 of the 15 hydrogen bonding elements in the peptide, one would expect its contribution to be about 20%. Moreover, the entire peptide in the lower leaflet forms more hydrogen bonds with the membrane host, and this peptide penetrates the membrane slightly less than its counterpart in the upper leaflet. Although we do not definitively present such a relationship here, our results suggest that peptide insertion is directly correlated with the extent of hydrogen bonding.

The TRP residue contains three hydrogen bonding elements: the hydrogen-accepting carbonyl of the backbone; the hydrogen-donating amide also of the backbone; and the hydrogen-donating nitrogen atom of the indole ring. The indole side chain appears to be primarily responsible for the hydrogen bonding of the TRP residue in both peptides, during most of the simulation (see Figure 3b). During the entire length of the simulation, this nitrogen heteroatom accounts for 81% of the hydrogen bonds formed between tryptophan and the membrane. This data suggests then that the indole ring contributes most significantly to the hydrogen-bonding potential of tryptophan, which in turn contributes to the hydrogen bonds formed between peptide and membrane. The prevalence of such hydrogen bonding between tryptophan and a membrane host has also been noted experimentally.[33] Thus, although hydrogen bonding alone does not explain the interfacial localization and stabilization, it is clear that the peptides hydrogen bond significantly with the membrane.

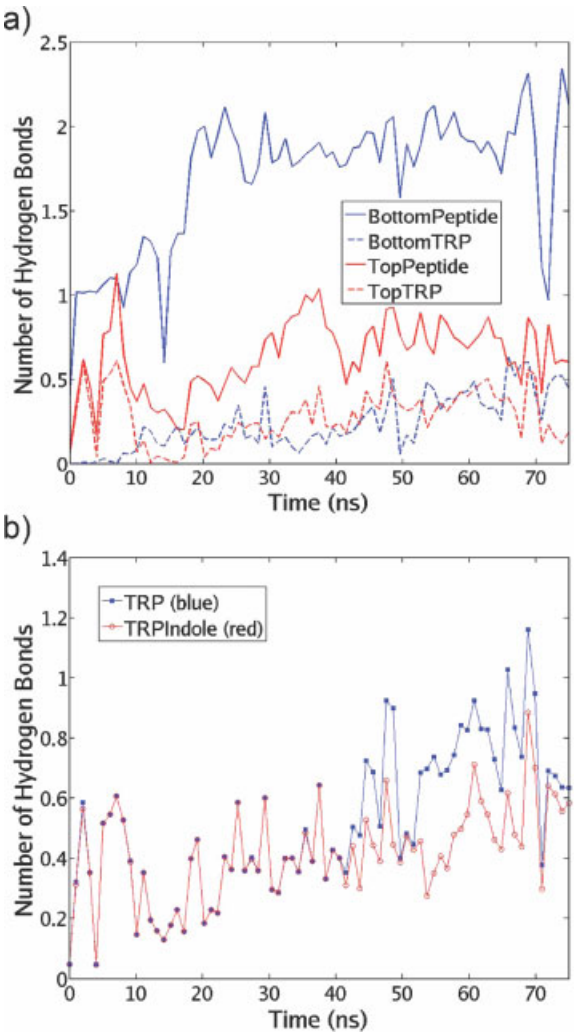

FIGURE 3 Average number of hydrogen bonds formed (over each ns of simulation). The cut-off criterion for hydrogen bonding was set to an angle of 30° and a radius of 0.3 nm. (a) Red and blue lines indicate profiles in the upper and lower membrane leaflets, respectively. Solid and dashed lines indicate hydrogen bonding between the membrane and the entire peptide or just the TRP residue, respectively. (b) Average number of hydrogen bonds between the indicated entity—either the entire TRP residue (blue squares) or just the indole side chain (red open circles)—and the DMPC membrane.

In addition to hydrogen bonding, the orientation of the indole ring is relevant for peptide localization and stabilization in a membrane host. We examine temporal variations in the angle between the plane of the indole ring and that of the membrane in both leaflets. As shown in Figure 4 (the dashed profiles), the orientation of the TRP indole rings fluctuates dramatically during the first half of the simulation but converges in the second half. During this last portion of the simulation, the average orientation angle of the indole ring in the upper leaflet is 26.2 ± 6.9° (averaged over blocks of 1 ns). That angle in the lower leaflet is 54.2 ± 6.8°. It appears that the most stable orientation angle of the indole ring in the membrane is neither 0° nor 90° but an intermediate value. Moreover, the fluctuation of the ring is small in magnitude (∼7°) thus demonstrating the constriction of the indole ring (at least with respect to its orientation angle). This is consistent with the previous discussion on the propensity of the indole ring to form hydrogen bonds. Because of its strong interactions with the membrane, the indole ring converges tightly to a particular orientation angle.

As the peptides insert, they are oriented parallel to the membrane plane. Following insertion, the peptides adopt a more tilted orientation during stabilization (see Figure 4, solid line profiles). This tilting can be rationalized in terms of thermodynamics; the preferred state of the hydrophobic leucine side chains is buried inside an apolar environment (the membrane core), while the preferred state of the indole ring is situated at the membrane interface. Thus, the indole ring acts as an anchor or a pivot point, about which the rest of the peptide rotates to insert into the membrane. In both leaflets, the peptide tilt angles converge to similar values. In the upper leaflet—as averaged over the last half of the simulation and in blocks of 1 ns—the tilt angle is 62.3 ± 4.3°. In the lower leaflet, the value is slightly larger at 73.8 ± 5.3°. These angles are comparable to experimentally-determined tilts. For example, Bradshaw et al. observed a tilt angle of 55° for a fusion peptide.[13]

If tilting is the result of a hydrophobic effect, what prevents the peptide from relaxing to a perpendicular conformation relative to the membrane plane (an angle of 0° in Figure 4)? Such an orientation would result in maximizing the hydrophobic interactions of the leucine residues, thus resulting in a presumably more favorable system. We suggest that hydrogen bonding plays a critical role here. In the lower leaflet, the peptide forms more hydrogen bonds with the membrane than in the upper leaflet (see Figure 3a). As a result, the tilt angle of the peptide in the lower leaflet is significantly greater, suggesting that the peptide is more parallel to the membrane plane. From these results, it appears that an increase in the number of hydrogen bonds causes the peptide to localize to the interface where it exhibits a parallel orientation.

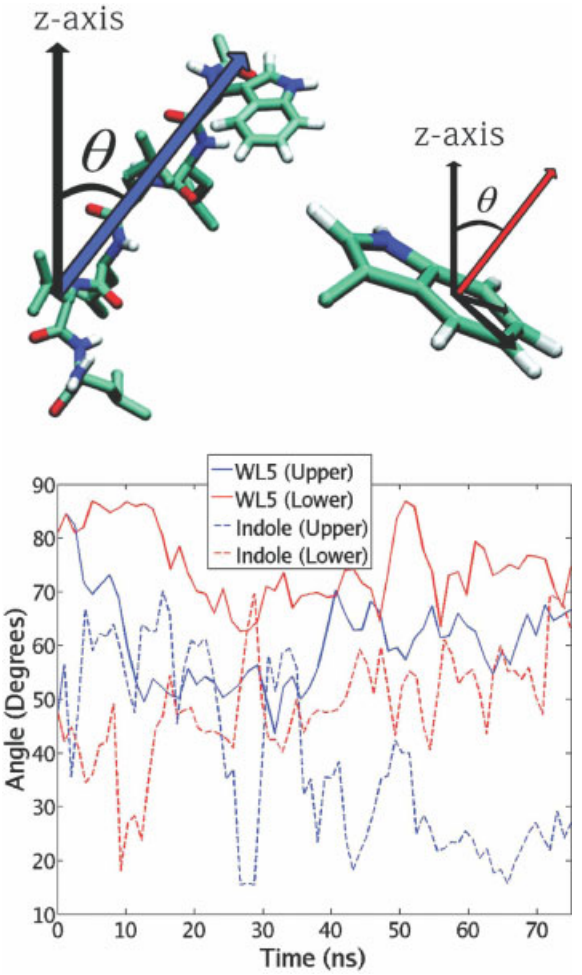

FIGURE 4 Orientation angles of the peptide and tryptophan side chain. Top panel of the figure describes the angles in question. Solid and dashed-line profiles represent the tilt of WL5 and the indole ring, respectively. Blue and red profiles depict the upper and lower leaflets, respectively. Data points are averaged over each ns of simulation.

Interestingly, the peptides acquire some secondary-structure characteristics as they insert and stabilize into the membrane (see Figure 5). The Ψ/Φ angles of the nonterminal residues of the peptides are localized in the upper left quadrant of the Ramachandran plot during the majority of the simulation. This quadrant is characteristic of β-sheet structure.[34] As averaged over 1 ns blocks during the entire simulation, the mean Φ of the internal residues is −110.2 ± 30.7°, while the mean Ψ is +110.3 ± 15.4°. These values contrast to those of the peptide in solution, prior to membrane insertion, during which we observe a broader distribution of Ψ/Φ values, varying by as much as 60° (data not shown). These results suggest that the membrane host restricts the atoms of the peptide backbone, such that the Ψ/Φ angle distribution is narrow and centered on the values consistent with β-sheet structure.

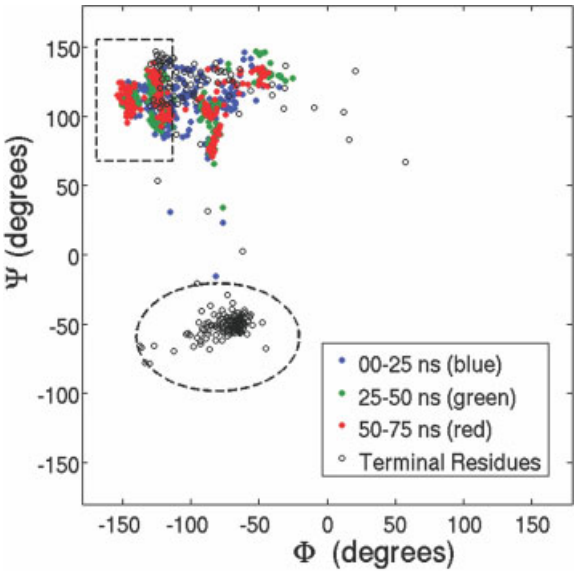

FIGURE 5 A Ramachandran plot, averaged over all of the nonterminal (colored dots) and terminal (open black circles) residues of both peptides and over 1 ns blocks. Blue, green, and red dots correspond to the beginning, middle, and end of the simulation, respectively. Terminal residues are shown over the entire simulation, clustering mostly in the region bound by the ellipse (non-β-sheet conformations). The nonterminal residues explore the upper-left quadrant, which is characteristic of β-sheet conformations (in particular, the boxed area).

Despite the evidence for β-sheet structure, the peptide is too small to form intramolecular secondary structure. However, such secondary structure can be achieved by the intermolecular interactions of several WL5 peptides. As observed by Wimley et al., multiple units of this model peptide (WL5) can assemble to form a larger β-barrel.[18] To probe the time scale of interaction between WL5 peptides, we examined their diffusion properties in the membrane plane. Figure 6 shows their displacement as a function of time. As a first approximation, the slope of the fit to these profiles ($\sim$6 Å^2/ns) yields information about the mobility of the peptides. Since the peptides do not significantly translate along the membrane normal after the insertion event, most of this displacement occurs in the membrane plane.

At a diffusion rate of approximately 6 Å^2/ns, and with a cross-sectional membrane area of about 3624 Å^2, the peptide should sample the entire membrane surface in approximately 600 ns. To approximate the time scale of interaction between two peptides in the same leaflet (not simulated here), it is critical to know the experimental concentrations of WL5 in the membrane. In one experiment, Wimley et al. use a peptide:lipid ratio of 2:100.[19] Extrapolating from our simulation here, a 100-lipid model membrane would occupy an area of 6000 Å^2. Two peptides migrating in this plane, at the aforementioned diffusion rate and assuming each peptide must cover only half of the area, could come into contact in approximately 0.5 μs. For this small model peptide to form a macromolecular assembly, the estimated time scale ($\sim$500 ns) is accessible by all-atom MD simulations, and we intend to study such associations in subsequent simulations.

Membrane Properties

The deuterium order parameters of the carbon atoms in the lipid tails provide insight into the physical properties of the membrane. Each order parameter, S_{CD}, is defined as

$$S_{CD} = 0.5\langle 3\cos^2\theta_n - 1\rangle$$

where θ_n is the angle between a vector along the methylene/methyl hydrogens of the carbon atom in question and the vector normal to the membrane plane.[15] For a particular carbon atom in a lipid tail, a larger order parameter correlates to minimal fluctuation in atomic location.

When modeling the insertion of a peptide into a membrane, the order parameters change as the insertion and stabilization events proceed (see Figure 7). The order parameters of nearly every carbon increase as a function of time. The most dramatic change can be noted when comparing the profile at 1 ns vs. 75 ns. It appears that the most statisti-

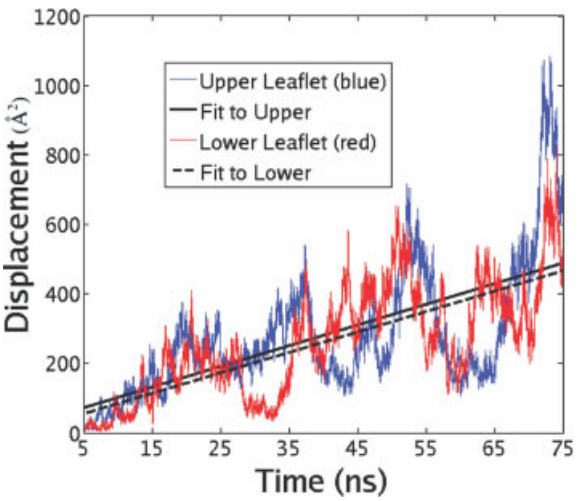

FIGURE 6 Displacement as a function of time, of the center of mass of the peptide in each leaflet. Reference coordinates are taken from a snapshot after 5 ns, when the peptides have inserted. Blue and red profiles correspond to the upper and lower leaflets of the membrane, respectively. Solid line is a linear fit to the blue profile, while the dashed line is a fit to the red profile. The slopes of both lines are approximately 6 Å^2/ns, and this is taken to be an approximate diffusion rate.

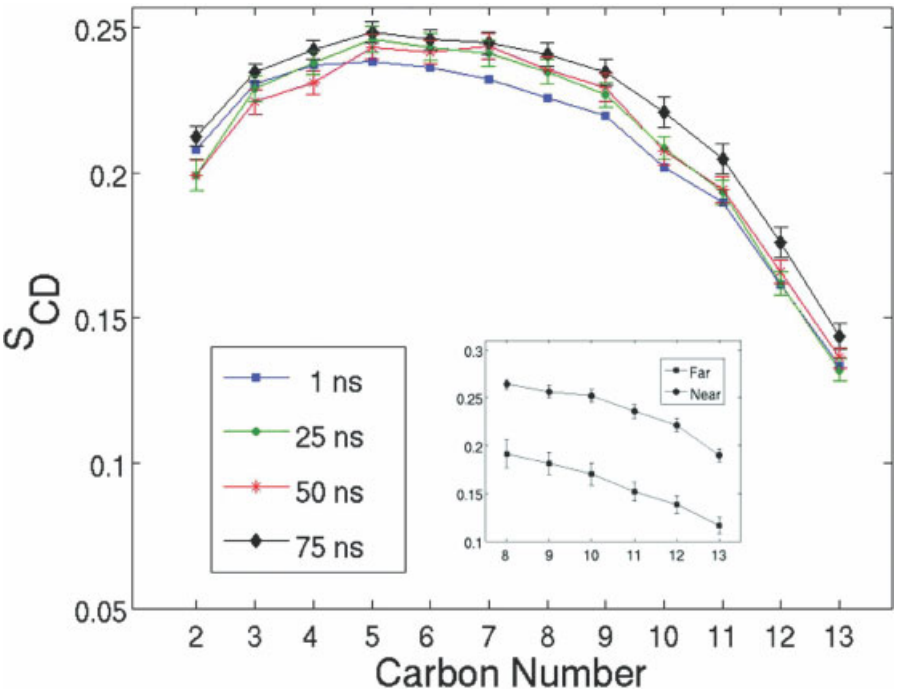

FIGURE 7 Deuterium lipid order parameters of the acyl chains in DMPC, shown at 1, 25, 50, and 75 ns of simulation (error bars are based on 1-ns block averages). Top and bottom leaflets were averaged together. Lower carbon numbers are those closer to the lipid head groups, while higher ones are those closer to the membrane core. The inset shows how the order parameters of the lipid carbon atoms differ near the peptide (within 10 Å, top curve, circles) and far from it (>10 Å, bottom curve, squares).

cally significant increase of the order parameters occurs in the lipid carbon atoms that reside near the membrane core (carbons 8–13). Thus, the insertion and stabilization of these peptides in the membrane has a slight ordering effect on the lipids. The cross-sectional area of the membrane was fixed via the dimensions of the simulation box. The thickness of the membrane, defined as the distance between the phosphorus atoms in the upper and lower leaflets also exhibited minimal change (see Figure 1). Thus, the ordering observed here is likely to originate from packing and constricting of the lipid carbon atoms, and this increased constriction may be a direct consequence of peptide insertion into the membrane.

The observed changes in membrane structure are likely local effects. In contrast, a global disruption of a biological membrane occurs primarily when numerous peptide units simultaneously insert and aggregate, as in the case of melittin.[35] We suggest that the observed ordering reported here is localized to the region surrounding the peptide. The inset of Figure 7 demonstrates this, where one can see that the lipid carbon atoms near the peptide (within 10 Å) are significantly raised. However, one should be careful in making any generalizations here; it is not always the case that a peptide raises order parameters in its vicinity. The exact effect of any membrane solute on the order parameters is probably a function of that solute's chemical nature and position. In any case, one can note that there is a significant perturbation to the order parameters, and that the change is a local one occurring near the peptide. Moreover, as found in our previous study, such a local effect can perturb the lateral pressure profile in the membrane.[36] Specifically, we observed that an embedded peptide changes the lateral pressure and increases the surface tension in the membrane. In turn, these effects can alter the physical properties of other transmembrane proteins, such as channel gates.[37]

In the discussion of transmembrane protein folding, it is often debated whether the transmembrane protein in question is shaped by the membrane, or whether the latter is perturbed by the former; indeed, there are several examples of both cases.[38–40] It is not surprising that the model membrane presented here can induce specific conformational changes in such a small peptide. It is especially intriguing that this small peptide can in turn cause significant changes to the membrane. Thus, as peptides insert and stabilize, the effect of small solutes on the membrane structure should not be neglected and may play a significant role in many biological processes.

CONCLUDING REMARKS

All-atom MD simulation results of the insertion, positioning, and stabilization of a small model peptide into a membrane have been presented here. The spontaneous insertion event is followed by a stabilization phase which is characterized by increased hydrogen bonding, restricted side chain orientation, and tilting of the peptide. We demonstrate how the tryptophan residue plays a crucial role during both the insertion and stabilization phases. Furthermore, we find that the membrane environment can induce significant secondary-structure conformations in the peptide WL5, while the peptide itself induces an ordering effect in the membrane. We also present a discussion about the mobility of the peptides in the membrane plane which affords a time scale for macromolecular assembly.

Interestingly, with respect to the tryptophan residue, a transmembrane protein does not always present its TRP residues at the membrane interface. Kelkar et al. discuss how some proteins—such as membrane channel or gating proteins—actually fluctuate their TRP residues from the interface to the membrane core. Such a fluctuation is related to their open and closed conformations and is thus not primarily driven by the interfacial preference of TRP. Although the interfacial location is likely the most thermodynamically stable position for TRP, the movement of the TRP residue away from the interface can have other structural and functional consequences.[41]

What then is the energetic cost of moving the TRP-containing segment of the protein (or in our case, just the entire model peptide) from the interface to the membrane core? This question has been addressed via simulation for just the indole side chain of TRP but not yet for an entire peptide.[42] In subsequent studies, employing the simulation techniques of nonequilibrium MD, we hope to calculate the energetics of WL5 movement across the membrane. Coupling these future simulation results with experimental data will allow us to further elucidate the details of transmembrane protein insertion, positioning, and stabilization.

REFERENCES

1. Taylor, C. W. Biochem J 1990, 272, 1–13.
2. Van der Wel, P. C. A.; Strandberg, E.; Killian, J. A.; Koeppe, R. E. Biophys J 2002, 83, 1479–1488.
3. Aruya, T.; Takeuchi, H. Biospectroscopy 1997, 4, 171–184.
4. Kim, J. E.; McCamant, D. W.; Zhu, L.; Mathies, R. A. J Phys Chem B 2001, 105, 1240–1249.
5. Caesar, C.; Esbjorner, E. K.; Lincoln, P.; Norden, B. Biochemistry 2006, 45, 7682–7692.
6. Im, W.; Brooks, C. L. PNAS 2004, 102, 6771–6776.
7. Bond, P.; Sansom, M. S. P. JACS 2006, 128, 2697–2704.
8. Stevens, M. J. J Chem Phys 2004, 121, 11942–11948.
9. Lopez, C. F.; Nielsen, S. O.; Srinivas, G.; DeGrado, W. F.; Klein, M. L. J Chem Theory Comput 2006, 2, 649–655.
10. Haider, S.; Grottesi, A.; Hall, B. A.; Ashcroft, F. M.; Sansom, M. S. P. Biophys J 2005, 88, 3310–3320.
11. Aliste, M. P.; Tieleman, D. P. BMC Biochemistry 2005, 6,30.
12. White, S. H.; Wimley, W. C. Nat Struct Biol 1996, 3, 842–848.
13. Bradshaw, J. P.; Darkes Malcom, J. M; Harroun, T. A.; Katsaras, J.; Epand, R. M. Biochemistry 2000, 39, 6581–6585.
14. Liu, W.; Caffrey, M. Biochemistry 2006, 45, 11713–26.
15. Gorfe, A. A.; Pellarin, R.; Caflisch, A. JACS 2004, 126, 15277–15286.
16. Stepaniants, S.; Izrailev, S.; Schulten, K. J Mol Model 1997, 3, 473–475.
17. Efremov, R. G.; Nolde, D. E.; Konshina, A. G.; Syrtcev, N. P.; Arseniev, A. S. Curr Med Chem 2004, 11, 2421–2442.
18. Wimley, W. C.; Hristova, K.; Ladokhin, A. S.; Axelsen, P. H.; White, S. H. J Mol Biol 1998, 277, 1091–1110.
19. Wimely, W. C.; White, S. H. J Mol Biol 2004, 342, 703–711.
20. Paul, C.; Wang, J.; Wimley, W. C.; Hochstrasser, R. M.; Axelsen, P. H. JACS 2004, 126, 5843–5850.
21. TriposTM, Inc.www.tripos.comSt. Louis, MO, USA.
22. Van Der Spoel, D.; Lindahl, E.; Hess, B.; Groenhof, G.; Mark, A. E.; Berendsen, H. J. C. J Comp Chem 2005, 26, 1701–1718.
23. http://moose.bio.ucalgary.ca/index.php?page=Structures_and_Topologies
24. Humphrey, W.; Dalke, A.; Schulten, K. J Mol Graph 1996, 14, 33–38.
25. Berger, O.; Edholm, O.; Jahnig, F. Biophys J 1997, 72, 2002–2013.
26. Darden, T.; York, D.; Pedersen, L. J Chem Phys 1993, 98, 10089–10092.
27. Essman, U.; Perera, L.; Berkowitz, M. L.; Darden, T.; Lee, H.; Pedersen, L. G. J Chem Phys 1995, 103, 8577–8593.
28. Berendsen, H. J. C.; Postma, J. P. M.; DiNola, A.; Haak, J. R. J Chem Phys 1984, 81, 3684–3690.
29. The MathWorks Inc, 1994–2006, http://www.mathworks. com/
30. Raudino, A.; Mauzerall, D. Biophys J 1986, 50, 441–449.
31. Huang, W.; Levitt, D. G. Biophys J 1977, 17,2, 111–128.
32. Cherstvy, A. G. J Phys Chem B 2006, 110, 14503–14506.
33. Yau, W.; Wimley, W. C.; Gawrish, K.; White, S. H. Biochemistry 1998, 37, 14713–14718.
34. Nelson, D. L.; Cox, M. M. Lehninger Principles of Biochemistry; Worth: New York, 2000; Chapter 6.
35. Hanke, W.; Methfessel, C.; Wilmsen, H. U.; Katz, E.; Jung, G.; Boheim, G. Biochem Biophys Acta 1983, 727, 108–114.
36. Gullingsrud, J.; Babakhani, A.; McCammon, J. A. Molec Simulat 2006, 32, 831–838.
37. Gullingsrud, J.; Schulten, K. Biophys J 2003, 85, 2087–2099.
38. Popot, J. L.; Engelman, D. M. Biochemistry 1990, 29, 4031–4037.
39. Pardo-Lopez, L.; Gomez, I.; Raussell, C.; Sanchez, J.; Soberon, M.; Bravo, A. Biochemistry 2006, 45, 10329–36.
40. Keifer, P. A.; Peterkofsky, A.; Guangshun, W. Anal Biochem 2004, 331, 33–39.
41. Kelkar, D. A.; Chattopadhyay, A. J Biosci 2006, 31, 1–6.
42. Norman, K. E.; Nymeyer, H. Biophys J 2006, 91, 2046–2054.

Reviewing Editor: Kenneth Breslauer.